JOURNAL OF AGRICULTURAL AND FOOD CHEMISTRY

Article

pubs.acs.org/JAFC

Use of Chemical and Physical Characteristics To Investigate Trends in Biochar Feedstocks

Fungai N. D. Mukome,[†] Xiaoming Zhang,[†] Lucas C. R. Silva,[†] Johan Six,[‡,§] and Sanjai J. Parikh*,[†]

[†]Department of Land, Air and Water Resources and [‡]Department of Plant Sciences, University of California Davis, Davis, California 95616, United States

[§]Department of Environmental Systems Science, ETH-Zurich, Zurich, Switzerland

Supporting Information

ABSTRACT: Studies have shown that pyrolysis method and temperature are the key factors influencing biochar chemical and physical properties; however, information on the nature of biochar feedstocks is more accessible to consumers, making feedstock a better measure for selecting biochars. This study characterizes physical and chemical properties of commercially available biochars and investigates trends in biochar properties related to feedstock material to develop guidelines for biochar use. Twelve biochars were analyzed for physical and chemical properties. Compiled data from this study and from the literature (n = 85) were used to investigate trends in biochar characteristics related to feedstock. Analysis of compiled data reveals that despite clear differences in biochar properties from feedstocks of algae, grass, manure, nutshells, pomace, and wood (hard- and softwoods), characteristic generalizations can be made. Feedstock was a better predictor of biochar ash content and C/N ratio, but surface area was also temperature dependent for wood-derived biochar. Significant differences in ash content (grass and manure > wood) and C/N ratio (softwoods > grass and manure) enabled the first presentation of guidelines for biochar use based on feedstock material.

KEYWORDS: *biochar, characterization, feedstock, C/N ratio, ash content, surface area*

INTRODUCTION

The presence of black carbon or "biochar" in the rich Terra Preta do Indio soils of the Amazon has resulted in the advancement of its use as a soil amendment,[1] and many agriculture practitioners are faced with the challenge of evaluating the benefits of applying biochar to their soil.[2] Despite the increasing research on this issue, at present there is a general lack of understanding of how biochar amendments will affect agroecosystem functioning.[3] Several benefits from the use of biochar have been reported, including improved water-holding capacity and nutrient retention,[1,4] increased soil fertility and agricultural production,[2,5,6] and greenhouse gas emission (GHG) reduction.[1,7] However, many studies have also shown opposing results, with no increase in crop yields, increased GHG emissions, and unintended elevation of soil pH.[3] These contrasting results are linked to the properties of the biochar used, application rate, soil type, and climate.[8]

Prior studies indicate that the pyrolysis method and temperature of pyrolysis are of great importance in determining biochar properties.[9−12] Operating conditions such as heating rate, highest treatment temperature (HTT), reaction vessel, chemical activation, and residence time have considerable influence on the properties of the biochar product; the HTT is considered to have the greatest effect on the physical properties of the biochar.[13,14] Unfortunately, due to the commercial and experimental nature of the newly developing biochar manufacturing industry, this information is often proprietary and hence not always available to biochar end-users.

Also of great importance to biochar properties is the feedstock used for biochar production, which has a substantial impact on the compositional constituents of the biochar. Many feedstocks including wood, sewage sludge, orange peels, rice husks, nutshells, pine shavings, manure, and straws[15,16] have been used to produce biochar. The wide variety of feedstocks is due to benefits associated with using locally available waste biomass, which limits transportation costs, airborne loss of product during transportation, and the overall carbon footprint of biochar production.

Although it has been argued that other factors such as soil type, soil chemistry, organic matter content, and climate[17] may be of greater importance to the agricultural impact of biochar incorporation, the importance of biochar feedstock cannot be overlooked.[18] The feedstock selected affects several properties with agronomic implications, including ash content (affects the soil mineral content),[19] the H/C ratio (approximates aromaticity of the biochar and is an indication of its ability to be mineralized),[20,21] pH (increases soil pH of acidic soils and affects mobility of ions in the soil),[11,19,22] surface area (helps predict CEC and possible sorption of GHGs),[3,13] and cation and anion exchange (may determine the potential for NH_4^+ and NO_3^- retention in N cycling).[11,17,19,23]

We propose that the chemical and physical characterization of biochar can provide valuable insight to end-users that are considering the use of a biochar for a particular agroecosystem. Although this has been proposed before, the results cannot be easily extrapolated due to the small sample size used.[19] Given the absence of standardized analytical methods for biochar characterization and the increase in commercially available

Received: August 30, 2012
Accepted: January 23, 2013
Published: January 23, 2013

ACS Publications © 2013 American Chemical Society

Table 1. Manufacturing Information and Physical Characteristics of 12 Commercially Available Biochars Analyzed in the Current Study

biochar	source material	pyrolysis temp (°C)	ash (wt %)	BET surface area (m^2/g)	type (hysteresis)
BC_ A	turkey litter	700−800	64	21.8	Ps. II[a] (H3)
BC_B[b]	walnut shell	900	40.4	227.1	Ps. II (H4)
BC_C	hardwood[c] + soil microorganism inoculation	370−520	15.5	95.9	Ps. II (H4)
BC_D	softwood[d]	600−700	2.4	25.2	Ps. II (H4)
BC_E	softwood + algal digestate	600−700	6.4	2	Ps. II (H3)
BC_F	softwood (mixed fir)[e]	510	3	165.8	Ps. II (H4)
BC_G	softwood (mixed fir)[e]	410	2.6	2.8	Ps. II (H3)
BC_H	softwood (pine)	500−650	17	4.9	Ps. II (H3)
BC_I	hardwood[c]	370−520	5	164.1	Ps. II (H4)
BC_J	hardwood (oak)	unavailable[f]	2.8	153.1	Ps. II (H4)
BC_K	hardwood	unavailable	5.5	154.4	Ps. II (H4)
BC_L	hardwood (cottonwood)	unavailable	4.2	301.6	Ps. II (H4)

[a]Ps.II, pseudo type II. [b]Not commercially available. [c]Mix of oak, maple, alder, white alder, black hawthorn, birch, cherry, black walnut, and lilac. [d]Mix of ponderosa pine, Douglas fir, larch, lodgepole pine, spruce, and alpine fir. [e]Predominately Douglas fir with some white fir. [f]Biochar distributor could not provide the exact pyrolysis temperature.

biochar, it would be valuable if different biochars could be evaluated on the basis of a simple measure such as feedstock, pyrolysis temperature, or pyrolysis method, thus avoiding potentially high costs of analyses. The primary objective of this study was to determine the chemical and physical characteristics of several commercially available biochars and use this information in conjunction with data from the biochar literature pool to determine if there are any evident trends that could be used as a guideline for end-users to assist in making informed decisions on biochar use.

MATERIALS AND METHODS

Safety. Respirators were worn during work with biochar with high ash content, and appropriate attire was used when ash content was determined using the muffle furnace.

Biochars. Twelve biochars from different feedstocks (Table 1) were obtained from various suppliers, sieved to pass through a 2 mm mesh, and analyzed for several chemical and physical properties. Additional information regarding the suppliers of biochars used is available in Appendix A of the Supporting Information. Several standard methods of soil analysis had to be modified for use on biochar, as properties such as buoyancy and hydrophobicity make centrifugation and wetting of biochar very challenging.

Physical Properties. *Ash Content.* ASTM E 1755-95 was used to determine the ash content.[24]

BET Surface Area. Surface area was measured via the Brunauer, Emmett, and Teller (BET) method that measures N_2 gas sorption (0.162 nm^2) at 77 K. Approximately 200 mg of ground biochar was outgassed at 120 °C for 16.5 h and then analyzed on an Autosorb-1 Surface Area Analyzer (Quantachrome Instruments). Five data points, with relative pressures of 0.05−0.3, were used to calculate the surface area.

Scanning Electron Microscopy. The surface morphology of the biochar was studied by scanning electron microscopy (SEM) using a Hitachi S-4100 FE-SEM operating at 5 kV. Sample preparation involved freeze-drying the samples for 3 days before they were adhered to aluminum stubs using graphite and nickel cement (Ted Pella, Redding, CA, USA).

Chemical Properties. *Elemental Analysis and pH.* An estimate of the percentage of elemental content was determined on an oven dry-weight basis by the University of California Davis Analytical laboratory (Davis, CA, USA) using microwave acid digestion of the samples followed by quantitative determination by ICP-AES. Determination of the H, C, and N contents was performed by Galbraith Laboratories, Inc. (Knoxville, TN, USA), and the O content was calculated by mass balance. The pH was measured in deionized water using a 1:2 or 1:3 (w/v) ratio with stirring and an equilibration time of 1 h. The pH was measured with an Orion 4 Star, Thermo Fisher Scientific pH-meter.

Cation Exchange Capacity (CEC). The CEC of the biochars was determined using a combination of the modified ammonium acetate compulsory displacement method[9,25] and rapid saturation diffusion method.[26] Briefly, 0.5 g of biochar samples contained in small plastic columns was leached under vacuum (−20 to −40 kPa) with deionized water five times followed by three washes with 5 mL of 1 M sodium acetate (pH 8.2) and three washes with 10 mL of 2-propanol. Samples were leached simultaneously using a SPE manifold (Fisherbrand PrepSep) equipped with luer fittings and 20 gauge (38 mm long) needles. The samples were vacuum-dried for 10 min after leaching with 2-propanol. Three washes of 10 mL with ammonium acetate (1 M, pH 7) were used to displace the sodium ions (Na^+), and the leachate was analyzed for Na^+ by atomic adsorption (PE 4100ZL, Perkin-Elmer, Waltham, MA, USA).

Total Surface Basicity and Acidity. The conventional back-titration method was used for this determination.[27] Approximately 0.20 g of biochar was soaked in 25 mL of 0.025 N HCl or NaOH solution (depending on analysis) in a centrifuge tube and agitated for 48 h at room temperature. The suspension was centrifuged, and the filtered supernatant was titrated with 0.025 N NaOH or HCl solution to determine the remaining of HCl or NaOH in solution.

ATR-FTIR and Raman. Surface functionality was investigated with a Thermo Nicolet 6700 spectrometer using a PIKE GladiATR single-bounce attenuated total reflection-Fourier transform infrared (ATR-FTIR) spectroscopy with a diamond internal reflection element (IRE) at ambient temperature (23 ± 1 °C). The spectra were collected in triplicate using a DTGS detector at 4 cm^{-1} resolution and 1.2 kHz scanning speed, for a total of 128 co-added scans. Raman analysis was performed on ground samples with a Renishaw RM1000 microscope (argon ion laser) at 514 nm. A power of 25 mW was used with an acquisition time of 30 s and a total of 5 scans per sample.

Statistical Analyses. The data from this study and from the literature were combined and analyzed using a one-way analysis of variance (ANOVA), with a $p < 0.05$ level of significance, to test for significant differences in ash contents, C/N ratios, and surface areas based on feedstock. The data were normalized by log transformation, and all analyses were performed using JMP software (version 10, SAS Institute Inc., Cary, NC, USA). If a difference existed, Tukey's honest significant difference (HSD) test was used to determine which treatments were different at the $p < 0.05$ level. Variations of the three properties with temperature based on feedstock were also investigated using least-squares regression. Ash content, C/N ratio, and surface area were selected for comparison due to availability of comparable data in the literature and also their agronomic importance. No surface area data for algal derived biochar were available in the literature, and therefore it was not included in the ANOVA.

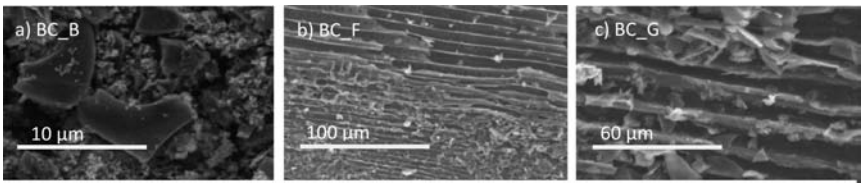

Figure 1. SEM images of selected biochars: (a) BC_B (walnut shell, 900 °C) with high ash content; (b) BC_F (softwood, 510 °C), which has a type H4 hysteresis loop; (c) BC_G (softwood, 410 °C), which has a type H3 hysteresis loop.

Table 2. Chemical Characteristics of the 12 Analyzed Biochars

char	C (wt %)	N (wt %)	C/N	H (wt %)	O (wt %)	PO_4-P (wt %)	K (wt %)	S (ppm)	Fe (ppm)	pH_w (1:2)	CEC[a] (cmol/kg)	acidity (mequiv/g)	basicity (mequiv/g)
BC_A	15.6	0.78	20.0	0.83	4.4	6.61	7.05	10720	9191	10.9	24.4	0.08	4.92
BC_B	55.3	0.47	117.7	0.89	1.6	0.64	9.32	940	1981	9.7	33.4		11.71
BC_C	53.3	1.96	27.2	3.70	24.3	0.47	1.2	5920	1109	6.8	44.5	1.22	1
BC_D	68.2	0.51	133.7	3.66	26.8	0.13	0.26	370	1934	7.5	26.2	1.24	1.02
BC_E	58.1	0.41	141.7	4.16	31.7	0.08	0.19	685	3370	6.8	67	1.56	1.22
BC_F	83.9	0.36	233.1	1.88	19.8	0.02	0.13	110	505	7.3	12	0.27	0.93
BC_G	65.7	0.21	312.9	4.38	23.5	0.02	0.12	50	248	7.1	10	0.83	0.4
BC_H	71.2	0.91	78.2	2.88	11.6	0.08	0.72	480	3517	7.9	3.2	0.79	1.01
BC_I	87.3	0.59	148.0	2.15	7.4	0.07	0.85	140	203	9.2	9.1	0.41	0.84
BC_J	88.0	0.44	200.0	2.55	14.8	0.02	0.33	60	79	9.5	14.9	0.49	0.87
BC_K	85.4	0.55	155.3	2.37	8.9	0.07	0.48	140	606	8.8	3.6	0.6	0.94
BC_L	82.5	0.49	168.4	1.64	5.6	0.06	1.02	160	473	9.5	16.5	0.36	1.21

[a]CEC, cation exchange capacity.

RESULTS

Biochar Characterization. The results from the characterization allowed for separation of the biochar into two main groups: wood- and non-wood-derived. Table 1 shows that wood-derived biochars have lower ash content (<7%) in comparison to non-wood-derived biochars, BC_A (64%) and BC_B (40%). The surface areas of the biochars ranged over 3 orders of magnitude with three of the biochars having surface areas of <5 m^2 g^{-1} (BC_A, BC_E, and BC_G), and the highest surface area was observed for BC_L (Table 1). The surface of the walnut shell biochar, which has the highest ash content and the second highest surface area (Table 1), consists mostly of plate-like structures with soot particles that contribute to its high surface area (Figure 1a). For wood-derived biochars, surface area correlates with pyrolysis temperature, with a low pyrolysis temperature corresponding to a low surface area. SEM micrographs reveal that the surface morphology of higher surface area (and temperature) biochars (Figure 1b) contain slit-shaped pores with vesicles, whereas lower surface area biochars (Figure 1c) show mostly plate-like particles with slit-shaped pores.

All biochars possess common characteristics of high pH (6.8−10.9) and high C/N ratio (>20) (Table 2). The non-wood-derived biochars have higher pH values, greater alkali/alkaline elements, and higher contents of total P (0.64 and 6.61% for BC_A and BC_B, respectively) and K (9.3 and 7.0% for BC_A and BC_B, respectively). Significant differences in the elemental content of C (15−88%), N (0.21−1.96%), O (1.6−31.7%), and H (0.83−4.38%) were also observed (Table 2), with clear separation of the biochars into wood- and non-wood-derived. There is a strong positive relationship between the H/C atomic ratios and the O/C atomic ratios of the biochars (Figure 2) consistent with van Krevelen diagrams.[3] Separation of feedstock groups was not distinct for CEC, with values ranging from 3.2 to 67 cmol kg^{-1} (Table 2). Biochars

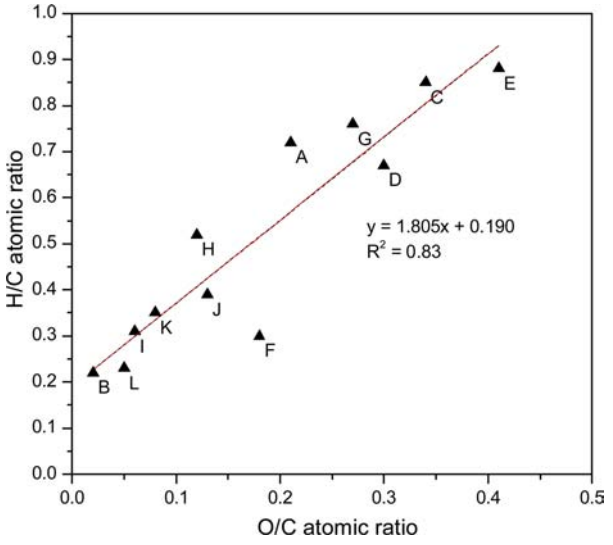

Figure 2. van Krevelen diagram of 12 biochars from the current study.

with additions of "enhancers," such as algae (BC_E) or beneficial soil microorganisms (BC_C), had increased CEC and surface acidity when compared to the wood biochars (BC_D, BC_F, BC_G, BC_J, BC_K, and BC_L). Surface acidity was most correlated with H and O content (R^2= 0.76 and 0.67, respectively), both of which are important in determining surface acid/base chemical activity. The surface basicity of BC_B (11.7 mequiv g^{-1}) was also much greater than for all the other biochars (Table 2).

Surface Functionality. Analysis of the ATR-FTIR spectra permitted separation of the biochar into the two groups, wood- and non-wood-derived, on the basis of the chemical functionality of the biochars (Figure 3). References for the band assignments are provided in Table 3. Only two peaks, at approximately 870 cm^{-1} (corresponding to lone aromatic C−H

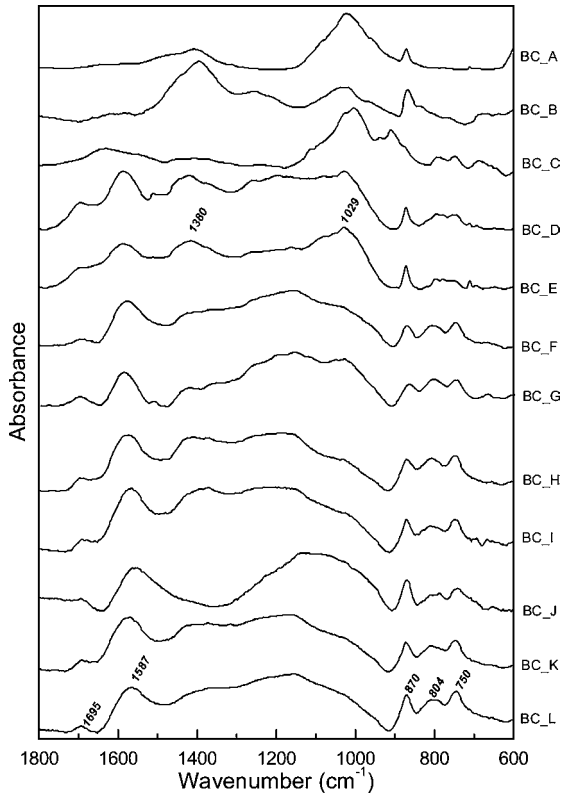

Figure 3. ATR-FTIR spectra of 12 biochars collected on a single-bounce diamond crystal.

out of plane vibration) and 1033 cm^{-1} (C−O symmetric stretch for O−CH_3 and C−OH), were common to the spectra of all samples. Other key peaks identified, particularly in the wood biochars, were aromatic C—H out of plane vibrations at approximately 723 and 797 cm^{-1}, aromatic C═C stretching vibration (a characteristic band of lignin) from 1560 to 1600 cm^{-1}, and C═O stretching between 1690 and 1710 cm^{-1} with the position of this peak being dependent on whether the C═O groups were in conjunction with the aromatic ring (below 1700 cm^{-1}) or not (above 1700 cm^{-1}). Another band identified between 1390 and 1420 cm^{-1} corresponds to aliphatic CH_3 deformations. To allow for comparison, the intensity of the peaks within each spectrum was normalized relative to the peak at 870 cm^{-1} (Table 4).

The Raman carbon first-order spectra of the biochars all exhibited two broad peaks centered at approximately 1650 cm^{-1} (G band) and 1350 cm^{-1} (D band) with sloping baselines (spectra not shown). Peak height ratios were used to calculate the I_D/I_G ratios (Table 4), and all of the wood biochars had higher ratios than the non-wood-derived biochars except for BC_G.

Data Analysis. A combination of data from the current study and that from the published literature for H/C versus O/C ratios (Figure 4), ash content (Figure 5a), C/N ratio (Figure 6a), and surface area (Figure 7a) reveals characteristic differences in these parameters based on biochar feedstock material (i.e., algae, grass, hulls, manure, shells, pomace, and wood; Table 5) The wood biochar was further separated into hard- and softwoods, to reveal significant differences in all three characteristics among the two feedstocks (Figures 5b, 6b, and 7b). Trends in ash content and C/N ratios supported by statistical differences at the $p < 0.05$ level (Appendix B, Supporting Information) of the biochars allowed for guidelines on the type of biochar to be selected on the basis of the potential agroecosystem effects of these properties (Table 6). A one-way ANOVA was peformed (Figure 8). The gray boxes show the range from second to third quartiles, with the median dividing the interquartile range into two boxes. Letters indicate significant differences ($p < 0.05$) according to Tukey's (HSD) multiple-means comparison. Although consistency of the data compiled from the literature was complicated by the current absence of standardized biochar analysis methods, analysis of data from compiled studies still exhibited significant separation by feedstock.

Except for pomace, no significant variation ($p < 0.05$) with temperature based on feedstock was determined for ash content and C/N ratio for any of the materials (Appendix C, Supporting Information). For surface area, only the hardwood- and softwood-derived biochars were significantly correlated with temperature.

Table 3. Functional Group Assignments Corresponding to Biochar Samples As Determined by ATR-FTIR Analysis

wavenumber (cm^{-1})	assignment	refs
2924	ν(C—H) vibrations in CH_3 and CH_2	40, 42−46
2850	ν(C—H) vibrations in CH_3 and CH_2	40, 42−46
1695	ν(C═O) vibration aromatic carbonyl/carboxyl C═O stretching	40, 42−46
1640	ν(C═C) vibration, C═C aromatic ring	40, 42−46
1587	skeletal C═C vibration	40, 42−46
1505−1515	skeletal C═C vibration (lignin)	40, 42−46
1460	δ(C—H) vibrations in CH_3 and CH_2	40, 42−46
1423	skeletal C═C vibration	40, 42−46
1380	ν(C—O) vibration aromatic and δ(C—H) vibrations in CH_3 and CH_{2v}	40, 42−46
1240−1260	ν(C—O) vibration phenolic	40, 42−46
1154	aromatic C—O stretching	42, 43, 45
1080−1040	S—O, C—O stretch of polysaccharides	42
1029	aliphatic ether C—O and alcohol C—O stretching	42−45
870	one adjacent H deformation	42−45
804	two adjacent H deformations	42−45
750	four adjacent H deformations	42−45
667	γ(OH) bend	42,45

Table 4. Infrared and Raman Spectral Analysis of Biochars

char	aromatic C−H (744 cm^{-1})[a]	aliphatic ether (1029 cm^{-1})[a]	aliphatic CH_3 (1380 cm^{-1})[a]	aromatic C=C (1587 cm^{-1})[a]	aromatic CO (1690 cm^{-1})[a]	Raman I_D/I_G[b]
BC_A		2.9	1	0.21	0.02	0.4
BC_B		1.1	2.2			0.34
BC_C	0.53	3.6	0.38	0.69	0.39	0.76
BC_D	0.63	2.67	2.46	2.6	1.2	0.58
BC_E	0.27	2.83	2.2	2.05	0.94	0.65
BC_F	1.2	2.09	1.7	2.3	0.28	0.4
BC_G	1.2	2.16	0.83	1.5	0.4	0.25
BC_H	1.12	1	1.71	1.78	0.41	0.83
BC_I	1	1.2	1.83	1.98	0.38	0.68
BC_J	0.71	1.67	0.27	1.41	0.36	0.72
BC_K	1.05	1.17	1.6	1.9	0.36	0.59
BC_L	1.1	1.01	1.05	1.22	0.12	0.71

[a]Ratios of peak intensities relative to the aromatic C−H stretch at 870 cm^{-1} common to all spectra. [b]Ratio of peak intensities of the carbon D (1350 cm^{-1}) and G (1690 cm^{-1}) bands in Raman spectra.

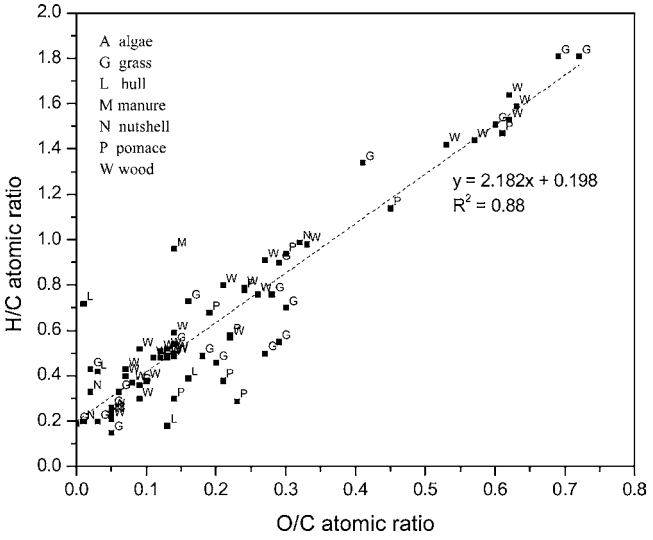

Figure 4. van Krevelen diagram of selected biochars from the literature.[7,10,16,20,27,39,42,44]

DISCUSSION

The study reveals that despite clear differences in biochar properties from feedstocks of algae, grass, manure, nutshells, pomace, and wood (hard- and softwoods), characteristic generalizations based on the feedstock can be made. It also shows that feedstock is a better predictor of variation in biochar ash content and C/N ratio than pyrolysis temperature. When one given feedstock is considered, temperature is the best predictor for surface area.

The majority of commercially available biochar is wood-derived[3] and, as expected, the ash content of wood-derived biochar was significantly lower than that of non-wood-derived biochar (Table 1), which is also consistent with prior studies.[9,19] The low ash content makes biochar from this feedstock more amenable to transportation and incorporation into soils, as there is less wind-blown loss. Selection of this type of biochar would also limit the increase in soil ash content, which has been associated with increased hydrophobicity[18] and causes potential retention of hydrophobic agrochemicals, such as the herbicide group of phenylureas.[28]

Biochar pH correlated best with O content (R^2 = −0.72), corroborating previous findings that biochar basicity resulted from oxygen-rich functional groups such as γ-pyrone-type, chromene, diketone, or quinone groups.[29] Although the oxygen content of feedstocks decreases with increasing pyrolysis temperature, the formation of compounds such as levoglucosan

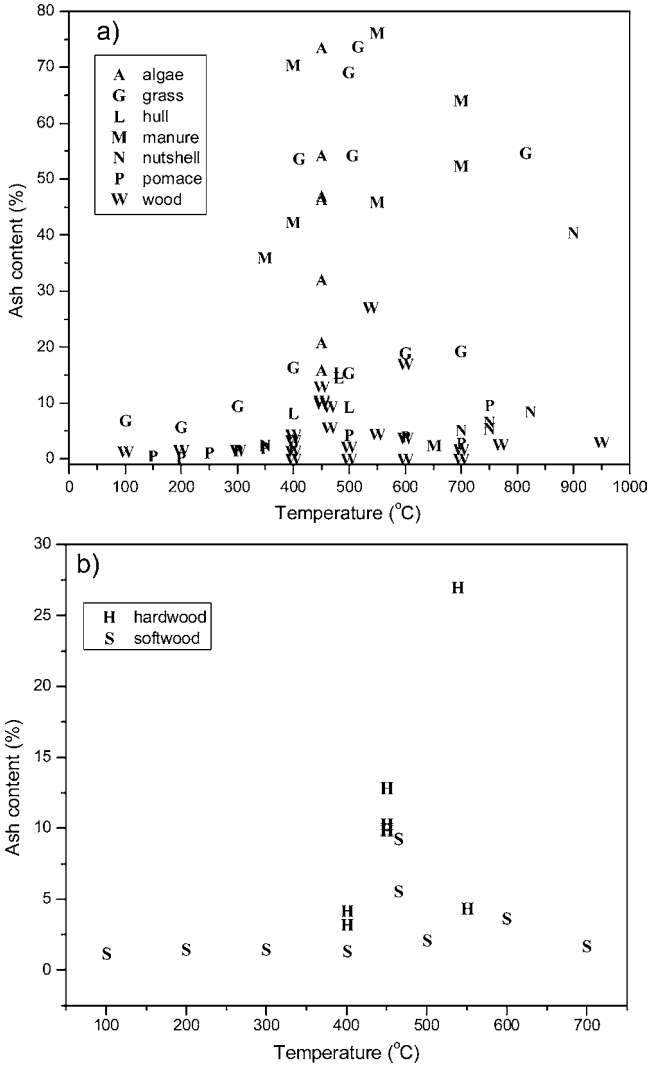

Figure 5. Change in ash content as a function of pyrolysis temperature of biochars derived from (a) various feedstocks (includes literature data; n = 97) and (b) hard- versus softwoods.

dx.doi.org/10.1021/jf3049142 | J. Agric. Food Chem. 2013, 61, 2196−2204

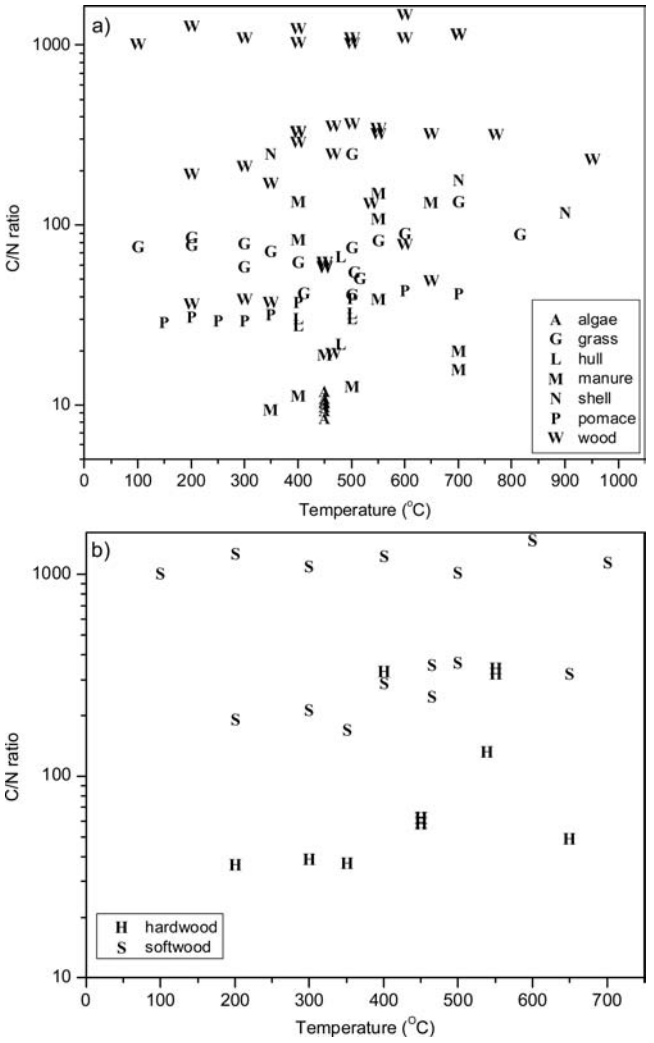

Figure 6. Change in the C/N ratio as a function of pyrolysis temperature of biochars derived from (a) various feedstocks (includes literature data; n = 97) and (b) hard- versus softwoods.

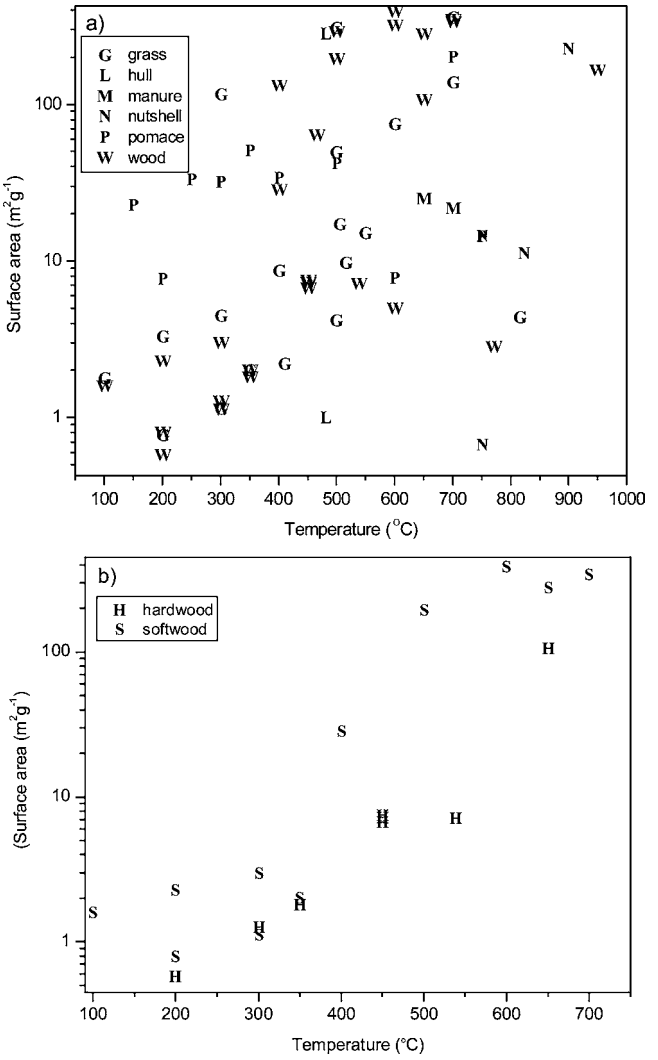

Figure 7. Change in BET surface area as a function of pyrolysis temperature of biochars derived from (a) various feedstocks (includes literature data; n = 97) and (b) hard- versus softwoods.

(from pyrolysis of cellulose material) and its byproducts (levoglucosenone, furfural, 2,3-butanedione, and 5-methylfurfural) results in oxygen-rich functional groups.[30] The basicity of the non-wood-derived biochar arises from the presence of salts, such as carbonates and chlorides of potassium and calcium in the ash.[29] This combination of increased basicity, which may be desirable for soils that require liming, and associated increased ash content, which is linked to mineral content and hydrophobicity, makes selection of a biochar for use as a soil amendment on the basis of any one specific characteristic challenging. Following an improved understanding of feedstock and pyrolysis conditions on biochar chemical and physical properties, methodical field trials are thus required to link biochar characteristics to soil fertility and crop production. With this combined data set, growers will be able to make informed decisions regarding selection of biochar. The BET surface area isotherms of the analyzed biochars were all type II (Table 1), consistent with ungraphitized black carbon surfaces.[31] Type II isotherms are associated with capillary nonporous or macroporous adsorbents and represent monolayer–multilayer adsorption. The differences were evident in the hysteresis loops with the biochars with lower surface areas (BC_A, BC_E, BC_G, and BC_H) exhibiting type H3 hysteresis loops.[32] The adsorption–desorption isotherms for these biochars closed before a relative pressure of <0.3 in the desorption process was reached, indicating a lack of microporosity. Furthermore, the type H3 hysteresis loops are evidence of aggregates of plate-like particles and slit-shaped pores giving rise to different paths of adsorption and desorption

Table 5. Guidelines of Biochar Characteristics Based on Feedstock

characteristic	observed trend
ash content	grass ≈ manure ≫ nutshells, pomace, and wood (hardwood > softwood)
C/N ratio	wood ≫ grass> pomace> manure (softwood > hardwood)
surface area	temperature dependent (softwood > hardwood)

Table 6. Potential Effects of Biochar Properties on Soil Quality

property	agroecosystem consideration
ash content	hydrophobicity and retention of agrochemicals
C/N ratio	initial immobilization of soil N
surface area	sorption of pesticides, herbicides, and heavy metals

dx.doi.org/10.1021/jf3049142 | J. Agric. Food Chem. 2013, 61, 2196–2204

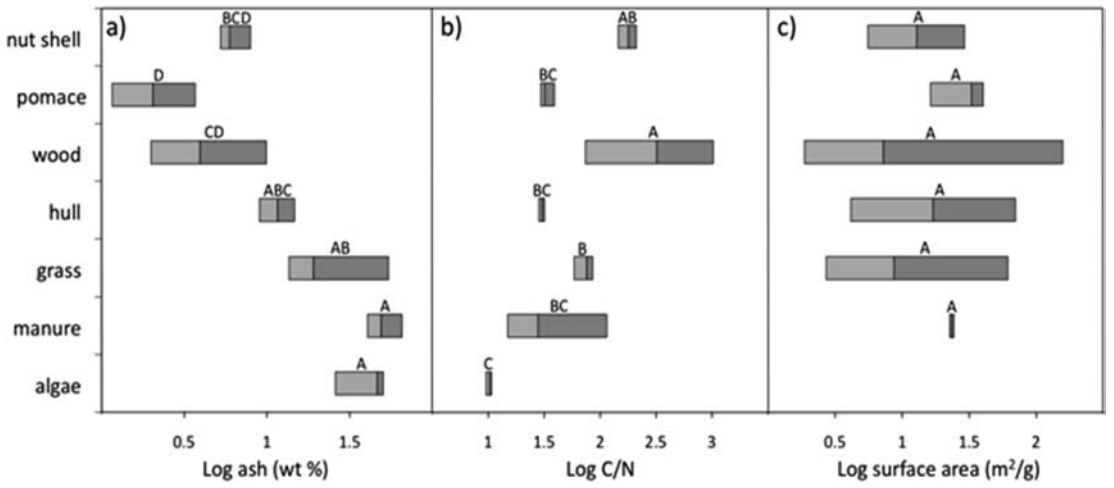

Figure 8. Box plots showing differences in (a) ash content and (b) C/N ratios and (c) BET surface area across different feedstocks. The gray boxes show the range from first to third quartiles, with the median dividing the interquartile range into two boxes for the second and third quartiles. Letters show significant differences ($p < 0.05$) according to a one-way ANOVA followed by Tukey's (HSD) multiple-means comparison.

of the N_2 gas.[32] This is consistent with the SEM images of the biochar (Figure 1c), which reveal plate-like particles.

The remaining biochars with higher surface area exhibited type H4 hysteresis loops associated with narrow slit-like pores.[32] The SEM images of the biochar exhibiting this hysteresis loop had slit-shaped pores from vesicles formed in the wood structure due to high-temperature pyrolysis (Figure 1b; BC_F). The presence of soot in BC_C, seen in the SEM image (Figure 1a), may also have contributed to the high surface area.[20,33] Soot has spherical microstructures of about 1 μm in diameter containing 90% C, giving it a high surface area.[34]

The FTIR spectra (Figure 3) of the study biochars showed considerable similarity in the aromatic functional groups present in the wood-derived biochars, with aromatic out of plane C—H bending vibrations (peaks between 700 and 900 cm^{-1}) associated with adjacent aromatic hydrogen bonds and aromatic C═C and C═O stretching vibrations (~1587 cm^{-1}) common to all of the studied biochars. Ratios of peak intensities relative to the aromatic C—H stretch at 870 cm^{-1} (Table 4) revealed significant differences in the wood- versus non-wood-derived biochar. Most notably, the non-wood biochars (BC_A and B) had less aromatic and greater aliphatic character than the wood biochars on the basis of the ratios of the peaks 870:1029 cm^{-1} (BC_A), 870:1417 cm^{-1} (BC_B), and 870:1587 cm^{-1} (BC_A and BC_B). The aliphatic character of a biochar is a good indicator of its susceptibility to rapid degradation by soil microorganisms,[2] with a greater aliphatic character resulting in rapid degradation and greater aromatic character signifying a more recalcitrant material. The H/C ratio, an approximation of aromaticity, decreased with increasing pyrolysis temperature (for example, BC_F vs BC_G) and agreed with the FTIR peak intensity ratios.

Consistent with high ratios of $CH:CH_3$ (870:1390 cm^{-1}), BC_A, BC_B, BC_D, and BC_E all had enhanced sloping of the baseline of their Raman spectra (spectra not shown). This phenomenon is associated with fluorescence from hydrogen-rich saturated aliphatic hydrocarbons.[35] The two bands in the Raman spectra arise from weak E_2g_1 vibrational modes (G band) and breathing modes of A_1g symmetry (D band). The I_D/I_G ratio has been used as an approximation for the ratio of sp^2/sp^3 carbons in disordered carbonaceous materials.[36]

A plot of the atomic H/C ratio to the atomic O/C ratio (van Krevelen diagram) for data collected in the current study (Figure 2) was consistent with a corresponding plot of biochars from the literature (Figure 4), decreasing with increasing temperature of production. As with biochar from the literature pool, the biochar from our study did not separate according to feedstock (Figure 2), showing that the processes responsible for the decreasing ratios, demethylation (H/C) and decarboxylation (O/C), are related more to temperature than to feedstock.

Distinguishing biochar as wood- and non-wood-derived is well established in the literature[3,15,37] and, until now, has been the primary metric of differentiation. Our characterization of biochar showed possibilities for greater differentiation, for example, differences between nutshell- and manure-derived biochar being very distinct. Analysis of ash content reveals that wood biochars consistently had lower ash content than the other feedstocks made at the same temperature (Figure 5a). This is consistent with a study by Singh et al.,[19] who observed lower ash content in eucalyptus-derived biochar compared to poultry litter and cow manure. Manure and grass biochars typically have higher ash contents due to the presence of silica from soil contamination (Figure 8). Differences within the wood-derived biochars were based on hardwood (maple, oak, and eucalyptus) versus softwoods (pine, Douglas fir, and cedar) feedstock, with the ash content of hardwood biochar generally being higher than for softwood biochar (Figure 5b). The ANOVA of the compiled literature data for ash content confirmed significant differences between the feedstocks (nutshell and algae/manure; grass and pomace/wood; wood and algae/manure) (Figure 8a).

A plot of the C/N ratio versus pyrolysis temperature of biochar from the literature pool showed separation based on feedstock (Figure 6a). In contrast to the ash content, the wood-derived biochar had higher C/N ratios than the non-wood-derived biochar for the same pyrolysis temperature. The C/N ratios, a good predictor for an organic material's capability for net N immobilization,[38] were all >20, suggesting the addition of the wood-derived biochar would result in a net N immobilization in the soil. The manure- and pomace-derived biochar had the lowest C/N ratios, with the grass-derived biochar having intermediate values. As before, the feedstock

correlation was consistent from low to high temperature. The large variability in the C/N ratios of the wood biochar was due to the difference in the C/N ratios of hard- and softwoods. The wood-derived biochar again separated into hard- and softwood, with higher ratios being observed in softwoods when compared to hardwoods (Figure 6b). In a study of decaying woody debris, Saunders et al.[39] observed that softwoods generally had higher C/N ratios than hardwoods. When data collected from the literature were examine (Figure 6b), a similar observation is made for biochars derived from hard- and softwoods; however, experiments tracking the C/N ratios of wood feedstocks through the pyrolysis process are required to establish causal links. Significant differences in C/N ratios were also confirmed by ANOVA ($p < 0.05$), with the wood biochar showing significant differences from all other biochars, except the nutshell-derived biochar (Figure 8b).

A similar plot investigating surface area did not reveal a clear trend associating biochar feedstock with surface area (Figure 7). However, there was a clear difference between the hardwood- and softwood-derived biochars: larger surface areas were observed for softwoods and increased with pyrolysis temperature, as observed in other studies (Figure 7b).[3,40] In a study comparing hard- and softwood charcoal, Darmstadt et al.[41] observed higher surface area for the softwoods than the hardwoods (maple) feedstock. The less dense composition of the softwoods renders them more susceptible to thermal decomposition, resulting in more vesicles and pores throughout the wood structure, which effectively increases the surface area. Surface area is mainly a function of pyrolysis temperature; hence, no significant differences were found among feedstocks (Figure 8c). Regression analysis of the compiled data also suggests that variation of surface area with temperature is feedstock dependent, due to the significant correlations seen for both hard- and softwoods but not the other feedstocks (Supporting Information).

This study demonstrates that differences and similarities between biochars can be identified on the basis of knowledge of the feedstock, and suggested guidelines for variation in biochar characteristics are given in Table 5. This is the first study to compile data from the biochar literature and suggests guidelines for biochar use based on feedstock as related to ash content, C/N ratio, and surface area, all properties with significant agroecosystem impact. This information has high potential value for biochar end-users who may be unable to test individual biochar samples prior to use as large-scale soil amendments. The international impetus to standardize biochar testing methods will assist in developing standardized data analyses enhancing additional comparative studies of other important biochar properties such as CEC, surface area, and acidity/basicity. Ideally, biochar end-users would be able to select a biochar feedstock for specific soil functions. The data presented here suggest that hardwood biochars will likely have a more basic pH and higher mineral content resulting in increased soil pH, whereas the softwood biochars will likely result in greater N immobilization and slower, more fungal-assisted decomposition, as well as potentially reduced N_2O emissions and nitrate leaching.

■ ASSOCIATED CONTENT

Supporting Information

Appendices with (A) information on biochar products and suppliers, (B) raw output data from one-way ANOVA, and (C) a table of the significance values of Pearson's correlation coefficients. This material is available free of charge via the Internet at http://pubs.acs.org.

■ AUTHOR INFORMATION

Corresponding Author

*E-mail: sjparikh@ucdavis.edu.

Funding

Funding was provided by the Agricultural Sustainability Institute (University of California, Davis) through a grant from the David and Lucile Packard Foundation.

Notes

The authors declare no competing financial interest.

■ ACKNOWLEDGMENTS

We thank Alan Hicklin for assistance with the Raman microscope at the NEAT-ORU, Thermochemistry Facility (University of California, Davis), and Dr. Thomas Young for access to the Quantachrome Autosorb-1.

■ ABBREVIATIONS USED

GHG, greenhouse gas; ANOVA, analysis of variance; ATR-FTIR, attenuated total reflectance Fourier transformed infrared spectroscopy; CEC, cation exchange capacity; HTT, highest treatment temperature; SEM, scanning electron microscopy; BET, Brunauer, Emmett, and Teller; ICP-AES, inductively coupled plasma atomic emission spectroscopy; DTGS, deuterated triglycine sulfate

■ REFERENCES

(1) Lehmann, J.; Gaunt, J.; Rondon, M. Bio-char sequestration in terrestrial ecosystems − a review. *Mitigation Adaptation Strategies Global Change* **2006**, *11*, 395−419.

(2) Van Zwieten, L.; Kimber, S.; Morris, S.; Chan, K.; Downie, A.; Rust, J.; Joseph, S.; Cowie, A. Effects of biochar from slow pyrolysis of papermill waste on agronomic performance and soil fertility. *Plant Soil* **2009**, *327*, 235−246.

(3) Lehmann, J.; Joseph, S. *Biochar for Environmental Management: Science and Technology*; Earthscan: London, UK, 2009.

(4) Glaser, B.; Lehmann, J.; Zech, W. Ameliorating physical and chemical properties of highly weathered soils in the tropics with charcoal − a review. *Biol. Fertil. Soils* **2002**, *35*, 219−230.

(5) Lal, R. Soils and food sufficiency: a review. *Sustainable Agric.* **2009**, 25−49.

(6) Laird, D. A.; Fleming, P.; Davis, D. D.; Horton, R.; Wang, B.; Karlen, D. L. Impact of biochar amendments on the quality of a typical Midwestern agricultural soil. *Geoderma* **2010**, *158*, 443−449.

(7) Singh, B. P.; Hatton, B. J.; Singh, B.; Cowie, A. L.; Kathuria, A. Influence of biochars on nitrous oxide emission and nitrogen leaching from two contrasting soils. *J. Environ. Qual.* **2010**, *39*, 1224−1235.

(8) Verhejien, F.; Jeddery, S.; Bastos, A.; van der Velde, C. M.; Diafas, I. *Biochar Application to Soils*; Institute for Environment and Sustainability, European Communities: Brussels, Belgium, 2010.

(9) Gaskin, J. W.; Steiner, C.; Harris, K.; Das, K. C.; Bibens, B. Effect of low-temperature pyrolysis conditions on biochar for agricultural use. *Trans. ASABE* **2008**, *51*, 2061−2069.

(10) Novak, J. M.; Lima, I. M.; Xing, B.; Gaskin, J. W.; Steiner, C.; Das, K. C.; Ahmedna, M.; Rehrah, D.; Watts, D. W.; Busscher, W. J.; Schomberg, H. Characterization of designer biochar produced at different temperatures and their effects on a loamy sand. *Ann. Environ. Sci.* **2009**, *3*, 195−206.

(11) Chan, K. Y.; Xu, Z. H. Biochar − nutrient properties and their enhancement. In *Biochar for Environmental Management: Science and Technology*; Lehmann, J., Joseph, S., Eds.; Earthscan: London, UK, 2009; pp 67−84.

(12) Brewer, C. E.; Schmidt-Rohr, K.; Satrio, J. A.; Brown, R. C. *Characterization of Biochar from Fast Pyrolysis and Gasification Systems*; Wiley: New York, 2009; Vol. *28*, pp 386−396.
(13) Lua, A. C.; Yang, T.; Guo, J. Effects of pyrolysis conditions on the properties of activated carbons prepared from pistachio-nut shells. *J. Anal. Appl. Pyrolysis* **2004**, *72*, 279−287.
(14) Downie, A.; Crosky, A.; Munroe, P. Physical properties of biochar. In *Biochar for Environmental Management: Science and Technology*; Lehmann, J., Joseph, S., Eds.; Earthscan: London, UK, 2009; pp 13−32.
(15) Spokas, K. A.; Reicosky, D. C. Impacts of sixteen different biochars on soil greenhouse gas production. *Ann. Environ. Sci.* **2009**, *3*, 179−193.
(16) Chen, B.; Chen, Z. Sorption of naphthalene and 1-naphthol by biochars of orange peels with different pyrolytic temperatures. *Chemosphere* **2009**, *76*, 127−133.
(17) Silber, A.; Levkovitch, I.; Graber, E. R. pH-dependent mineral release and surface properties of cornstraw biochar: agronomic implications. *Environ. Sci. Technol.* **2010**, *44*, 9318−9323.
(18) Kookana, R. S.; Sarmah, A. K.; Van Zwieten, L.; Krull, E.; Singh, B. Chapter 3: Biochar Application to Soil: Agronomic and Environmental Benefits and Unintended Consequences. In *Advances in Agronomy*; Donald, L. S., Ed.; Academic Press: San Diego, CA, 2011; Vol. *112*, pp 103−143.
(19) Singh, B.; Singh, B. P.; Cowie, A. Characterisation and evaluation of biochars for their application as a soil amendment. *Aust. J. Soil Res.* **2010**, *48*, 516−525.
(20) Hammes, K.; Smernik, R. J.; Skjemstad, J. O.; Schmidt, M. W. I. Characterisation and evaluation of reference materials for black carbon analysis using elemental composition, colour, BET surface area and ^{13}C NMR spectroscopy. *Appl. Geochem.* **2008**, *23*, 2113−2122.
(21) Krull, E. S.; Baldock, J. A.; Skjemstad, J. O.; Smernik, R. J. Characteristics of biochar: organo-chemical properties. In *Biochar for Environmental Management: Science and Technology*; Lehmann, J., Joseph, S., Eds.; Earthscan: London, UK, 2009.
(22) Rondon, M.; Lehmann, J.; Ramírez, J.; Hurtado, M. Biological nitrogen fixation by common beans (*Phaseolus vulgaris* L.) increases with bio-char additions. *Biol. Fertil. Soils* **2007**, *43*, 699−708.
(23) Liang, B.; Lehmann, J.; Solomon, D.; Kinyangi, J.; Grossman, J.; O'Neill, B.; Skjemstad, J. O.; Thies, J.; Luizão, F. J.; Petersen, J.; Neves, E. G. Black carbon increases cation exchange capacity in soils. *Soil Sci. Soc. Am. J.* **2006**, *70*, 1719−1730.
(24) Firestone, M. K.; Firestone, R. B.; Tiedje, J. M. Nitrous oxide from soil denitrification: factors affecting its biological production. *Science* **1980**, *208*, 749−751.
(25) Sumner, M. E.; Miller, P. W. Cation exchange capacity and exchange coefficients. In *Methods of Soil Analysis*; SSSA and ASA: Madison, WI, 1996; pp 1201−1230.
(26) Mulvaney, R. L.; Yaremych, S. A.; Khan, S. A.; Swiader, J. M.; Horgan, B. P. Use of diffusion to determine soil cation-exchange capacity by ammonium saturation. *Commun. Soil Sci. Plant Anal.* **2004**, *35*, 51−67.
(27) Jindarom, C.; Meeyoo, V.; Kitiyanan, B.; Rirksomboon, T.; Rangsunvigit, P. Surface characterization and dye adsorptive capacities of char obtained from pyrolysis/gasification of sewage sludge. *Chem. Eng. J.* **2007**, *133*, 239−246.
(28) Sopeña, F.; Semple, K.; Sohi, S.; Bending, G. Assessing the chemical and biological accessibility of the herbicide isoproturon in soil amended with biochar. *Chemosphere* **2012**, *88*, 77−83.
(29) Montes-Morán, M. A.; Suárez, D.; Menéndez, J. A.; Fuente, E. On the nature of basic sites on carbon surfaces: an overview. *Carbon* **2004**, *42*, 1219−1225.
(30) Kawamoto, H. M., M.; Saka, S. Pyrolysis behavior of levoglucosan as an intermediate in cellulose pyrolysis: polymerization into polysaccharide as a key reaction to carbonized product formation. *J. Wood Sci.* **2003**, *49*, 469−473.
(31) Sing, K. S. W. Physisorption of gases by carbon blacks. *Carbon* **1994**, *32*, 1311−1317.
(32) Sing, K. S. W. Reporting physisorption data for gas/solid systems with special reference to the determination of surface area and porosity. *Pure Appl. Chem.* **1982**, *54*, 2201−2218.
(33) Akhter, M. S.; Chughtai, A. R.; Smith, D. M. The structure of hexane soot I: spectroscopic studies. *Appl. Spectrosc.* **1985**, *39*, 143−153.
(34) Goldberg, E. D. *Black Carbon in the Environment*; Wiley: New York, 1985.
(35) Marshall, C. P.; Javaux, E. J.; Knoll, A. H.; Walter, M. R. Combined micro-Fourier transform infrared (FTIR) spectroscopy and micro-Raman spectroscopy of Proterozoic acritarchs: a new approach to palaeobiology. *Precambrian Res.* **2005**, *138*, 208−224.
(36) Casiraghi, C.; Ferrari, A. C.; Robertson, J. Raman spectroscopy of hydrogenated amorphous carbons. *Phys. Rev. B* **2005**, *72*, 085401.
(37) Novak, J. M.; Reicosky, D. C. Impacts of sixteen different biochars on soil greenhouse gas production. *Ann. Environ. Sci.* **2009**, *3*, 179−193.
(38) Stevenson, F. J.; Cole, M. A. *Cycles of Soil − Carbon,Nitrogen, Phosphorus, Sulfur, Micronutrients*; Wiley: New York, 1999.
(39) Saunders, M. R.; Fraver, S.; Wagner, R. G. Nutrient concentration of down woody debris in mixedwood forests in central Maine, USA. *Silva Fennica* **2011**, *45*, 197−210.
(40) Keiluweit, M.; Nico, P. S.; Johnson, M. G.; Kleber, M. Dynamic molecular structure of plant biomass-derived black carbon (biochar). *Environ. Sci. Technol.* **2010**, *44*, 1247−1253.
(41) Darmstadt, H.; Pantea, D.; Sümmchen, L.; Roland, U.; Kaliaguine, S.; Roy, C. Surface and bulk chemistry of charcoal obtained by vacuum pyrolysis of bark: influence of feedstock moisture content. *J. Anal. Appl. Pyrolysis* **2000**, *53*, 1−17.
(42) Hsu, J.-H.; Lo, S.-L. Chemical and spectroscopic analysis of organic matter transformations during composting of pig manure. *Environ. Pollut.* **1999**, *104*, 189−196.
(43) Sharma, R. K.; Wooten, J. B.; Baliga, V. L.; Lin, X.; Geoffrey Chan, W.; Hajaligol, M. R. Characterization of chars from pyrolysis of lignin. *Fuel* **2004**, *83*, 1469−1482.
(44) Özçimen, D.; Ersoy-Meriçboyu, A. Characterization of biochar and bio-oil samples obtained from carbonization of various biomass materials. *Renewable Energy* **2010**, *35*, 1319−1324.
(45) Wu, H.; Yip, K.; Tian, F.; Xie, Z.; Li, C.-Z. Evolution of char structure during the steam gasification of biochars produced from the pyrolysis of various mallee biomass components. *Ind. Eng. Chem. Res.* **2009**, *48*, 10431−10438.
(46) Brewer, C. E.; Schmidt-Rohr, K.; Satrio, J. A.; Brown, R. C. Characterization of biochar from fast pyrolysis and gasification systems. *Environ. Prog. Sustainable Energy* **2009**, *28*, 386−396.

NOTE ADDED AFTER ASAP PUBLICATION

This paper published February 19, 2013 with errors in Figure 6 and Figure 8. The correct version published February 22, 2013.